

## 2ν Double Beta Decay and Self-Consistent Self-Energies

D. B. Stout<sup>(a)</sup> and T. T. S. Kuo

Physics Department, State University of New York at Stony Brook, Stony Brook, New York 11794-3800

(Received 24 February 1992)

We have performed quasiparticle-random-phase-approximation (QRPA) calculations of the  $\nu\nu$  transition matrix for  $^{76}\text{Ge}$ ,  $^{82}\text{Se}$ , and  $^{100}\text{Mo}$ , using effective interactions derived from the Paris and the Bonn  $NN$  potentials. Unlike earlier QRPA calculations where the self-energy corrections to the single-particle spectra were suppressed, we have retained these corrections as given by our interactions. In this way our calculations are able to avoid the commonly encountered difficulty of QRPA instability near  $g_{pp}=1$ . The  $M^{2\nu}$  matrix elements of  $^{76}\text{Ge}$ ,  $^{82}\text{Se}$ , and  $^{100}\text{Mo}$  given by our calculation, with no adjustable parameters, are in reasonably good agreement with recent direct counter experiments.

PACS numbers: 23.40.Hc, 21.60.Jz, 27.50.+e, 27.60.+j

Although the lepton-number-violating neutrinoless double beta decay has yet to be observed, thanks to some new and impressive experiments [1-4], an increasing number of nuclei have been observed to undergo the two-neutrino double beta decay predicted by the standard model.

The two-neutrino decay half-life [5-7] may be written as  $T_{1/2}^{2\nu} = S_{2\nu}/M^{2\nu}$ , where  $S_{2\nu}$  contains the phase-space factors, and  $M^{2\nu}$  is the nuclear transition matrix element (usually approximated by the Gamow-Teller contribution  $M_{GT}^{2\nu}$ ). For use in the quasiparticle-random-phase-approximation (QRPA) formalism,  $M_{GT}^{2\nu}$  may be written as

$$M_{GT}^{2\nu} = \sum_n \sum_{a,b} \sum_{c,d} \frac{\langle 0_f^+ | \{a_{\pi_a}^\dagger a_{\nu_c}\}^{J^+} | 1_n^+ \rangle \langle 1_n^+ | \{a_{\pi_b}^\dagger a_{\nu_d}\}^{J^+} | 0_i^+ \rangle \langle a | \sigma | c \rangle \langle b | \sigma | d \rangle}{(E_n - E_i + Q_{\beta\beta}/2 + m_e)(2J+1)}, \quad (1)$$

where the particle-hole angular momentum quantum number has  $J=1$ .  $E_n - E_i$  is the nuclear excitation energy of the intermediate states,  $m_e$  is the mass of the electron, and  $Q_{\beta\beta}$  is the double-beta-decay  $Q$  value.  $a, b$  ( $c, d$ ) are summed over all possible proton (neutron) single-particle (s.p.) states. Note that we only need sum over  $1^+$  intermediate nuclear states.

To calculate the above nuclear transition matrix element, we need to know the respective nuclear wave functions and energies. One usually obtains such information from model-space effective interactions  $V_{\text{eff}}$ . It is a common practice to employ some empirical  $V_{\text{eff}}$  such as a delta interaction. Another approach is to derive  $V_{\text{eff}}$  from modern free nucleon-nucleon interactions such as the Paris [8] and Bonn [9,10] potentials. There have been a number of calculations deriving such  $V_{\text{eff}}$  for light nuclei [11,12]. For heavy double-beta-decay nuclei, such calculations become much more difficult. Staudt, Kuo, and Klapdor-Kleingrothaus have used  $G$ -matrix effective interactions derived from the above potentials in QRPA  $\beta\beta$  calculations for  $^{76}\text{Ge}$  [13] and for  $^{128}\text{Te}$  and  $^{130}\text{Te}$  [14]. Their results of the  $2\nu$  matrix elements  $M_{GT}^{2\nu}$  for these nuclei are, however, considerably higher than the respective experimental values.

In this work we shall perform  $2\nu\beta\beta$  decay calculations for  $^{100}\text{Mo}$ ,  $^{82}\text{Se}$ , and  $^{76}\text{Ge}$  using a QRPA framework, with the required effective interaction  $V_{\text{eff}}$  derived from the Paris and Bonn nucleon-nucleon potentials. A main difference between our present calculation and earlier ones concerns the self-energy corrections to the s.p. spectrum. As to be discussed later, these self-energy corrections will turn out to be very important for the  $2\nu$  matrix

elements. They are calculated and retained in the present work, while in earlier calculations they were suppressed, assuming that their effects were already contained in the empirical Woods-Saxon s.p. spectrum.

A well-known difficulty in earlier  $2\nu\beta\beta$  calculations is that the calculated  $M_{GT}^{2\nu}$  matrix elements were frequently unstable with respect to a particle-particle interaction strength parameter  $g_{pp}$  in the vicinity of its physical value, i.e.,  $g_{pp}=1.0$ . We shall see later that our present calculation no longer seems to have this undesirable trouble.

The effective interaction used in the present work is calculated from a  $QTQ$   $G$  matrix defined by the equation [11]

$$G_T(\omega) = V + VQ_{2p} \frac{1}{Q_{2p}(\omega - T)Q_{2p}} Q_{2p}G_T(\omega), \quad (2)$$

where  $Q_{2p}$  is the two-particle (2p) projection operator for all such states lying outside the model space. A  $Q_{2p}$  projection operator specified by  $(n_1, n_2, n_3) = (6, 15, 28)$  [13,14] is used in the present work. We numerically solved the above equation according to the formally exact technique of Tsai and Kuo [11,15].

The pairing force is in large part responsible for the occurrence of double beta decay. To take pairing into account, we follow the BCS theory and solve the familiar gap equations [16],

$$\Delta_a = (2j_a + 1)^{-1/2} \sum_c (2j_c + 1)^{1/2} u_c v_c (-1)^{l_c} G(aacc0), \quad (3)$$

where  $\Delta_a$  is the pairing gap and  $v_a^2$  the occupation proba-

bility ( $u_a^2 + v_a^2 = 1$ ) for a given s.p. state  $a$ . The particle-particle interaction  $G$  is defined

$$G(abcdJ) \stackrel{\text{def}}{=} -\frac{1}{2} (1 + \delta_{ab})^{1/2} \times (1 + \delta_{cd})^{1/2} \langle abJM | \hat{V}_{\text{eff}} | cdJM \rangle. \quad (4)$$

The self-energy is given by

$$\mu_a = 2(2j_a + 1)^{-1} \sum_{bj} (2J + 1) v_b^2 G(ababJ), \quad (5)$$

and the quasiparticle energy  $E_a$  is defined as

$$E_a \stackrel{\text{def}}{=} [(\varepsilon_a - \mu_a - \lambda)^2 + \Delta_a^2]^{1/2}, \quad (6)$$

where  $\varepsilon_a$  is the bare s.p. spectrum, and  $\lambda$  the chemical potential.

The above are a set of self-consistent equations, to be solved within a set of chosen active orbits. For example, in our present calculation the active orbits are the nine orbits in the  $0f1p$  and  $0g1d2s$  shells. They are the valence orbits outside the  $^{40}\text{Ca}$  core, and hence the bare s.p. energies  $\varepsilon$  are those corresponding to the situation of only one valence nucleon outside the  $^{40}\text{Ca}$  core. Evidently  $\mu$  represents the self-energy correction to the s.p. energies due to the interaction with other active nucleons.

In earlier calculations one tried to determine  $\mu$  empirically, by treating the combined quantity  $\varepsilon - \mu$  as the experimental or empirical s.p. energies. The intention is to determine  $\mu$  more reliably, since the effective interaction used may not be accurate enough and thus the calculated  $\mu$  may have a large uncertainty. There is, however, a subtle point. The  $pn$  QRPA framework is employed in the present work, as in earlier calculations. Within this framework the above BCS equations are solved for protons and for neutrons separately and independently; the interaction between protons and neutrons does not enter either. Let us consider  $^{100}_{42}\text{Mo}_{58}$  as an example. We use an active space consisting of nine proton orbits and nine neutron orbits outside the  $^{40}\text{Ca}$  core. Thus  $^{100}\text{Mo}$  has 22 active protons and 38 active neutrons. When one solves the proton BCS equation, the index  $b$  of Eq. (5) is summed over only the nine proton orbits with the sum of  $(2j_b + 1)v_b^2$  normalized to 22. The neutron orbits do not enter Eq. (5). Hence  $\mu_a$  represents the interaction of proton  $a$  with all the other active protons only. In other words,  $\mu$  contains the self-energy corrections only among the active protons. Hence the quantity  $\varepsilon - \mu$  here does not correspond to the experimental proton s.p. energies in  $^{100}\text{Mo}$ , which contain not only proton-proton but also neutron-proton interactions among the sixty active nucleons outside the  $^{40}\text{Ca}$  core. The situation for the neutron BCS equation is the same.

Thus the usual procedure, adopted in earlier QRPA calculations (see, for example, [13,14,17-19]), of setting  $\mu$  equal to zero and at the same time replacing  $\varepsilon$  by the empirical Woods-Saxon s.p. energies such as those for  $^{100}\text{Mo}$  is in fact somewhat debatable. Presumably the Woods-Saxon s.p. energies contain the interaction between one particular nucleon and all the other 99 neutrons and protons, which is not consistent with the BCS

framework as discussed above. For the latter, the s.p. energies  $\varepsilon$  should contain only the interaction with the forty neutrons and protons in the  $^{40}\text{Ca}$  core.

A less controversial and more straightforward procedure would be to calculate  $\mu$  as given by the BCS equations and use the s.p. energies as defined by the nuclear core,  $^{40}\text{Ca}$  in the present case, consisting of s.p. orbits below those included in the  $pn$  QRPA calculation. We have chosen this procedure, and have noticed that the results of these two approaches are importantly different.

In Fig. 1, we compare the neutron s.p. spectra given by the above two approaches. On the right-hand side of the figure we plot a Woods-Saxon neutron spectrum appropriate for  $^{100}\text{Mo}$ . The left-hand side is our calculated  $\varepsilon - \mu$  spectrum. We also display our calculated  $\lambda$ , or Fermi surface. Note that the positions for the  $g_{9/2}$ ,  $g_{7/2}$  levels are quite different for the two spectra. Also the present spectrum has a generally larger energy spread. Our results are obtained as follows. The bare s.p. energies  $\varepsilon_a$  are taken from those corresponding to a  $^{40}\text{Ca}$  core, which are deduced mainly from experiment [20,21]. Then the BCS equations for  $^{100}_{42}\text{Mo}$  are solved using a Paris-force  $G$  matrix calculated via the techniques described above and a model space containing the  $fp$  and  $gds$  shells.

These BCS results are then used in a standard  $pn$  QRPA secular equation where parameters  $g_{pp}$  and  $g_{ph}$  are introduced [13,14]. The former parameter adjusts the strength of the particle-particle interaction which enters the  $pn$  QRPA equation, and similarly the latter for the particle-hole interaction. When using realistic effective interactions one should use of course  $g_{pp} = g_{ph} = 1$ . The stability of the QRPA equation with respect to the interaction strengths may, however, be tested by artificially varying the strength parameters  $g_{ph}$  and  $g_{pp}$  in the vicini-

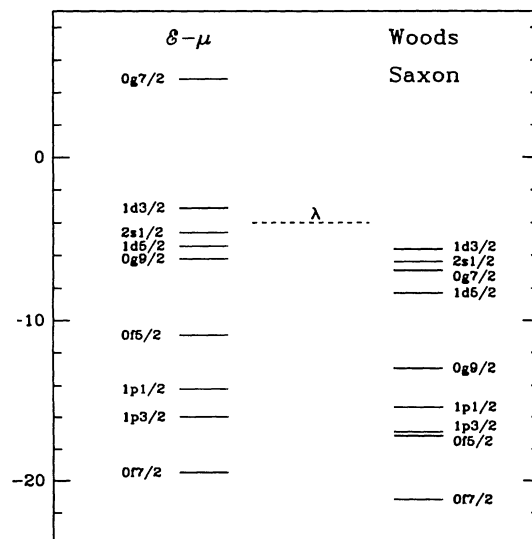


FIG. 1. Effect of self-energy on neutron single-particle spectrum for  $^{100}\text{Mo}$ .

ty of 1. We note for future reference that the QRPA eigenvectors obey the orthogonality relation  $X_\alpha^* X_\beta - Y_\alpha^* Y_\beta = 0$  for  $\alpha \neq \beta$ . Their normalization is taken as  $X_\alpha^* X_\alpha - Y_\alpha^* Y_\alpha = 1$ . (It has been pointed out, however [22], that this normalization is not always appropriate within a model-space framework.)

We now present our results for QRPA calculations of two-neutrino transition matrix elements  $M_{GT}^{2\nu}$  [13]. As a first calculation, we use as the effective interaction our model space bare  $G$  matrices calculated with the Paris potential. A plot of  $M_{GT}^{2\nu}$  vs  $g_{pp}$  with  $g_{ph}=1$  is shown in Fig. 2(a) (we only vary  $g_{pp}$  since QRPA calculations to date show a greater sensitivity to the parameter  $g_{pp}$  than  $g_{ph}$ ). Curve II was obtained by replacing the BCS-calculated s.p. energies,  $\epsilon_a - \mu_a$ , with the Woods-Saxon energies. Curve I was obtained by using the s.p. spectrum  $\epsilon_a - \mu_a$ , where  $\epsilon_a$  is a  $^{40}\text{Ca}$  s.p. spectrum, and  $\mu_a$  is the calculated self-energy obtained from (5). The experimentally derived matrix element  $M_{exp}^{2\nu}$  is denoted by a circle plotted at  $g_{pp}=1$ . As we cannot know the sign of  $M_{exp}^{2\nu}$ , we plot the circle at  $\pm M_{exp}^{2\nu}$ .

The rather dramatic dip in curve II is due to the fact that near  $g_{pp}=1$ , QRPA breaks down and contains unphysical complex solutions. One may readily verify from the structure of the QRPA matrix [13] that QRPA eigenvectors must satisfy

$$(w_m^* - w_n)(X_m^* X_n - Y_m^* Y_n) = 0. \quad (7)$$

For regions containing only real eigenvalues, this yields

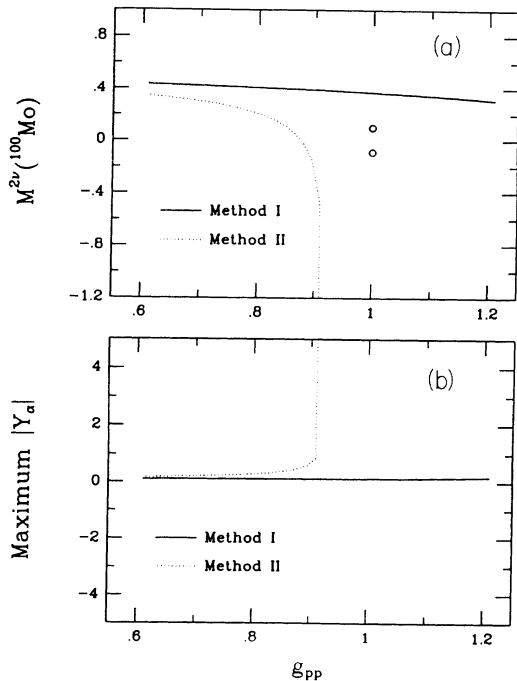


FIG. 2. (a)  $M_{GT}^{2\nu}$  calculated for  $^{100}\text{Mo}$  with (curve I) the calculated  $\epsilon - \mu$  single-particle spectrum, and (curve II) a Woods-Saxon single-particle spectrum. (b) Maximum  $|Y_a|$  vs  $g_{pp}$ . Bare Paris  $G$  matrix is used.

the familiar RPA orthogonality relations. It does not, however, specify RPA eigenvector normalizations. For complex eigenvalues, (7) requires  $X_m^* X_m - Y_m^* Y_m = 0$ . This means that near the onset of complex eigenvalues, at least one of the QRPA eigenvectors has the property that  $|Y_a| \rightarrow |X_a|$ . Thus as we approach the onset of complex QRPA eigenvalues, the usual QRPA eigenvector normalization condition  $|X_a|^2 - |Y_a|^2 = 1$  causes the normalizations  $|X_a|$  and  $|Y_a|$  for at least one state,  $a$ , to individually diverge and dominate the contributions to  $M_{GT}^{2\nu}$ . To emphasize this point, we plot in Fig. 2(b) the maximum  $|Y_a|$  vs  $g_{pp}$ . Thus the rather dramatic behavior of  $M_{GT}^{2\nu}$  in curve II is therefore not surprising.

We point out that the existence of a region of complex eigenvalues is not a surprise, and that essentially all QRPA equations would yield complex eigenvalues for sufficiently large values of  $g_{pp}$ . It is simply the presence of complex eigenvalues in the physical  $g_{pp}=1$  region that prevents us from extracting meaningful results from calculation II. In curve I, we use the calculated  $\epsilon - \mu$  s.p. energies as discussed above. In this case, we find that the region of complex QRPA eigenvalues lies a comfortable distance beyond the physical  $g_{pp}=1$  regime. This is important, since as we see in Fig. 2(b) calculation I does not contain unphysically large  $|Y_a|$  normalizations. We also note that curve I lies relatively close to the matrix element deduced from experiment. This agreement is rather encouraging considering the rather large cancellations involved in the calculation of  $M_{GT}^{2\nu}$ .

As a result of its improved performance with regard to QRPA-induced stabilities, we shall use from now on the

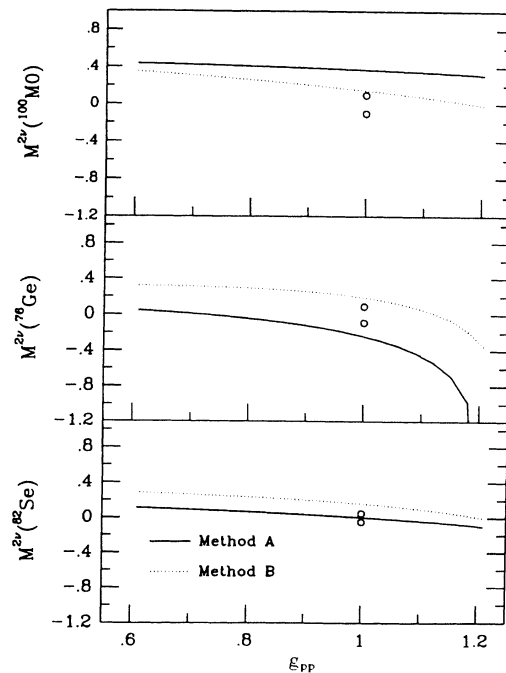


FIG. 3. Calculated  $M_{GT}^{2\nu}$  as a function  $g_{pp}$  for the Paris potential. Curve A with bare  $G$ , and B with  $G + G_{3ph}$ .

s.p. energies corresponding to curve I in the calculation of  $M_{GT}^{2\nu}$ . In Fig. 3 we display  $M_{GT}^{2\nu}$  vs  $g_{pp}$  for  $^{100}\text{Mo}$  using the Paris potential for two approximations to the effective interaction. Curve A is calculated with the bare  $G$  matrix only. Curve B is calculated including the bare  $G$  matrix and the core-polarization diagrams (i.e., diagram  $G_{3p1h}$  of Ref. [11]). Starting from the same set of bare s.p. energies and using the same treatment for the self-energies, we have also calculated  $^{76}\text{Ge}$  and  $^{82}\text{Se}$  using the Paris potential. Results are also displayed in Fig. 3 with quite similar behavior. We note that in all three cases the experimental value lies within or close to the range demarcated by the bare and bare plus core polarization curves. We have repeated the above calculations using the Bonn potential, and obtained results which are quite similar to Fig. 3.

The use of effective interactions derived from the Paris and Bonn potentials has also been investigated by Staudt, Kuo, and Klapdor-Kleingrothaus [13,14] for calculations involving tellurium and germanium, but with a Woods-Saxon treatment of the s.p. spectrum. Although they find that when including renormalization corrections, the region of complex eigenvalues occurs for  $g_{pp} > 1$ , their predicted matrix elements are  $\sim 4$  times larger than experiment. In this work we employed a different treatment for the s.p. spectrum; we retain the self-energies as derived from the BCS theory. We recall from Fig. 1 that our self-consistent spectrum and the Woods-Saxon one have small but qualitatively important differences. Apparently these differences have changed the QRPA  $M_{GT}^{2\nu}$  results in a dramatic way. For all three nuclei we considered,  $^{76}\text{Ge}$ ,  $^{82}\text{Se}$ , and  $^{100}\text{Mo}$ , we started from the same set of bare  $^{40}\text{Ca}$  s.p. energies. And for all three cases we see that the calculated matrix elements exhibit a fairly weak dependence on  $g_{pp}$ , up to and slightly above  $g_{pp} = 1$ . A persistent difficulty in earlier calculations of  $M_{GT}^{2\nu}$  for  $^{100}\text{Mo}$  is its particularly strong dependence on  $g_{pp}$  in the vicinity of  $g_{pp} = 1$ . It seems that this difficulty is alleviated by our present treatment of the s.p. self-energies.

As far as we know, most earlier QRPA calculations have imposed a shift to the calculated excitation energy spectra so that the calculated lowest  $1^+$  excitation energies coincide with the experimental values. This shift is not imposed in our present calculations. We have found that our results are not significantly changed if such a shift is included. In fact our calculation does not contain any adjustable parameters.

In summary, we presented results of  $2\nu\beta\beta$  calculations using the quasiparticle-random-phase-approximation method with model-space  $V_{\text{eff}}$  derived from the Paris and Bonn nucleon-nucleon potentials. The BCS calculations were performed for the nuclei  $^{76}\text{Ge}$ ,  $^{82}\text{Se}$ , and  $^{100}\text{Mo}$  using an  $f$ - $p$  and  $g$ - $d$ - $s$  shell-model space with the inner  $^{40}\text{Ca}$  shells treated as a closed core. We have used a  $^{40}\text{Ca}$  s.p. spectrum with the self-energies  $\mu$  calculated and retained. We showed that the choice of a Woods-Saxon

s.p. spectrum made by other authors would lead in our calculation to complex QRPA eigenvalues in the physical regime, which is perhaps a main cause for the often encountered QRPA instability in the vicinity of  $g_{pp} = 1$ . We presented our results, which are in fact all rather close to experimentally obtained  $2\nu$  matrix elements for  $^{76}\text{Ge}$ ,  $^{82}\text{Se}$ , and  $^{100}\text{Mo}$ .

The authors would like to thank Dan Strottman for his help in developing the large model-space  $G$ -matrix codes. We also thank Petr Vogel, H. V. Klapdor-Kleingrothaus, A. Staudt, and X. R. Wu for many helpful discussions. This work was supported in part by U.S. DOE Grant No. DE-FG02-88ER40388.

- (a)Current address: Division de Physique Theorique, Institut de Physique Nucléaire, 91406 Orsay CEDEX, France.
- [1] S. R. Elliot, A. A. Hahn, and M. K. Moe, *Phys. Rev. Lett.* **59**, 2020 (1987); in *Proceedings of the International Workshop on Neutrino Physics, Heidelberg, October 1987*, edited by H. V. Klapdor and B. Povh (Springer, Berlin, 1988), p. 213; in *Neutrino '88*, edited by J. Schneps *et al.* (World Scientific, Singapore, 1989).
  - [2] H. Ejiri *et al.*, *Phys. Lett. B* **258**, 17 (1991).
  - [3] A. A. Vasenko *et al.*, *Mod. Phys. Lett. A* **5**, 1299 (1990).
  - [4] H. S. Miley *et al.*, *Phys. Rev. Lett.* **65**, 3092 (1990).
  - [5] W. C. Haxton and G. Stephenson, Jr., *Prog. Part. Nucl. Phys.* **12**, 409 (1984).
  - [6] M. Doi *et al.*, *Prog. Theor. Phys. Suppl.* **83**, 1 (1985).
  - [7] T. Tomoda, *Rep. Prog. Phys.* **54**, 53 (1991).
  - [8] R. Vinh-Mau, in *Mesons in Nuclei*, edited by M. Rho and D. Wilkenson (North-Holland, Amsterdam, 1979), p. 151.
  - [9] R. Machleidt, K. Holinde, and C. Elster, *Phys. Rep.* **149**, 1 (1987).
  - [10] R. Machleidt, *Adv. Nucl. Phys.* **19**, 189 (1989).
  - [11] E. M. Krenciglowa, C. L. Kung, T. T. S. Kuo, and E. Osnes, *Ann. Phys. (N.Y.)* **101**, 154 (1976).
  - [12] M. F. Jiang, R. Machleidt, D. B. Stout, and T. T. S. Kuo, *Phys. Rev. C* **40**, R1857 (1989).
  - [13] A. Staudt, T. T. S. Kuo, and H. V. Klapdor-Kleingrothaus, *Phys. Lett. B* **242**, 17 (1990).
  - [14] A. Staudt, T. T. S. Kuo, and H. V. Klapdor-Kleingrothaus, *Phys. Rev. C* **46**, 871 (1992).
  - [15] S. F. Tsai and T. T. S. Kuo, *Phys. Lett.* **38B**, 427 (1972).
  - [16] T. T. S. Kuo, E. U. Baranger, and M. Baranger, *Nucl. Phys.* **79**, 513 (1966).
  - [17] K. Grotz and H. V. Klapdor, *Nucl. Phys.* **A460**, 395 (1986).
  - [18] P. Vogel and M. R. Zirnbauer, *Phys. Rev. Lett.* **57**, 3148 (1986).
  - [19] O. Civitarese, A. Faessler, and T. Tomoda, *Phys. Lett. B* **194**, 11 (1987).
  - [20] N. Vinh-Mau, *Nucl. Phys.* **A491**, 246 (1989).
  - [21] C. Gregoire, T. T. S. Kuo, and D. B. Stout, *Nucl. Phys.* **A530**, 94 (1991).
  - [22] S. D. Yang and T. T. S. Kuo, *Nucl. Phys.* **A456**, 413 (1986).